Quaternary International xxx (xxxx) xxx–xxx

Contents lists available at ScienceDirect

Quaternary International

journal homepage: www.elsevier.com/locate/quaint

The linkages with fires, vegetation composition and human activity in response to climate changes in the Chinese Loess Plateau during the Holocene

Zhihai Tan[a,b,*], Yongming Han[a,e], Junji Cao[a], Chun Chang Huang[c], Longjiang Mao[d], Zhao Liu[b], Zhisheng An[a]

[a] State Key Laboratory of Loess and Quaternary Geology, Key Laboratory of Aerosol Chemistry and Physics, Institute of Earth Environment, Chinese Academy of Sciences, Xi'an, Shaanxi 710075, PR China

[b] Department of Environment & Chemical Engineer, Xi'an Polytechnic University, Xi'an, Shaanxi 710048, PR China

[c] Department of Geography, Shaanxi Normal University, Xi'an, Shaanxi 710062, PR China

[d] School of Marine Science, Nanjing University of Information Science & Technology, Nanjing, Jiangsu 210044, PR China

[e] School of Human Settlements and Civil Engineering, Xi'an Jiaotong University, Xi'an, Shaanxi 710049, PR China

ARTICLE INFO

Keywords:
Black carbon
Charcoal
Holocene
Human activities
Vegetation composition

ABSTRACT

Holocene paleo-records of the Chinese Loess Plateau loess–soil profiles were used to reconstruct wildfire patterns and landscape evolution. We examine black carbon and charcoal influx, combined with the Magnetic susceptibility, $\delta^{13}C$ values of soil organic matter, pollen counts and other paleo-environmental proxies to discuss interactions with biomass–climate during the Holocene. The history of fires from the charcoal and black carbon (BC, char and soot) influx at the two sites demonstrates a transition from climate-controlled low amplitude variations with peaks during the Early and Middle Holocene (11-3.1kyearsB.P.) to higher amplitude variability in fire occurrence decoupled from climate and tied to human activities during the Late Holocene (3.1-0kyearsB.P.). The difference in fire patterns was attributed to regional effective moisture and human land use over the entre Loess Plateau; meanwhile, fire activities observed during the Holocene are consistent with variations in vegetation composition inferred from $\delta^{13}C$ values in soil organic matter, pollen counts, and paleoclimate proxies. Regional wildfires rarely occurred on the desert steppe dominated by a weedy C_3 taxon (*Artemisia, Compositae,* and *Chenopodiaceae* dominated)during the late glacial period. A limited biomass would not meet fire propagation in the extreme colder and drier environment of the Loess Plateau during those periods, though. As the climate became ameliorated during the early Holocene, there was an increasing biomass and a sufficient contribution do to high fuel accumulation from C_4 taxon (*Gramineae*). As the middle Holocene progressed toward warmer and wetter conditions, fire events were less frequent on the steppe and forest-steppe (e.g. expansion of trees C_3,*Quercus, Corylus*) of the Loess Plateau. Subsequently, the number of local and regional fire events have largely increased with the colder and drier climate conditions (e.g. expansion of C_3 weedy), which have been decoupling with intensive anthropogenic burning for farming since the past 3kyr.

These data suggests that the regional fire patterns vary strongly along environmental gradients in the effective moisture and regional fuel availability as well as the spatial and temporal distributions of Neolithic burning practices over the Loess Plateau in response to the weakening East Asian monsoon during the Holocene.

1. Introduction

Fires play a key role in the evolution of the natural landscape and in the carbon cycle from the terrestrial biosphere to the atmosphere (Bowman et al., 2009). The extent and frequency of wildfires are closely related to seasonal climate variability (wet or dry), vegetation types and human activity (Conedera et al., 2009). The occurrence of fire is largely controlled by climatic changes (Archibald et al., 2008), and thus influenced by vegetation structure and productivity (Daniau et al., 2009; Pechony and Shindell, 2010); Fire occurrence in turn responded to climate condition through the evolution of vegetation and post-fire response at the millennium timescales (Moreira et al., 2011).

* Corresponding author. State Key Laboratory of Loess and Quaternary Geology, Key Laboratory of Aerosol Chemistry and Physics, Institute of Earth Environment, Chinese Academy of Sciences, Xi'an, Shaanxi 710075, PR China.

E-mail addresses: tonishtan@163.com (Z. Tan), Cao@loess.llqg.ac.cn (J. Cao).

https://doi.org/10.1016/j.quaint.2018.03.041
Received 30 March 2016; Received in revised form 23 October 2017; Accepted 29 March 2018

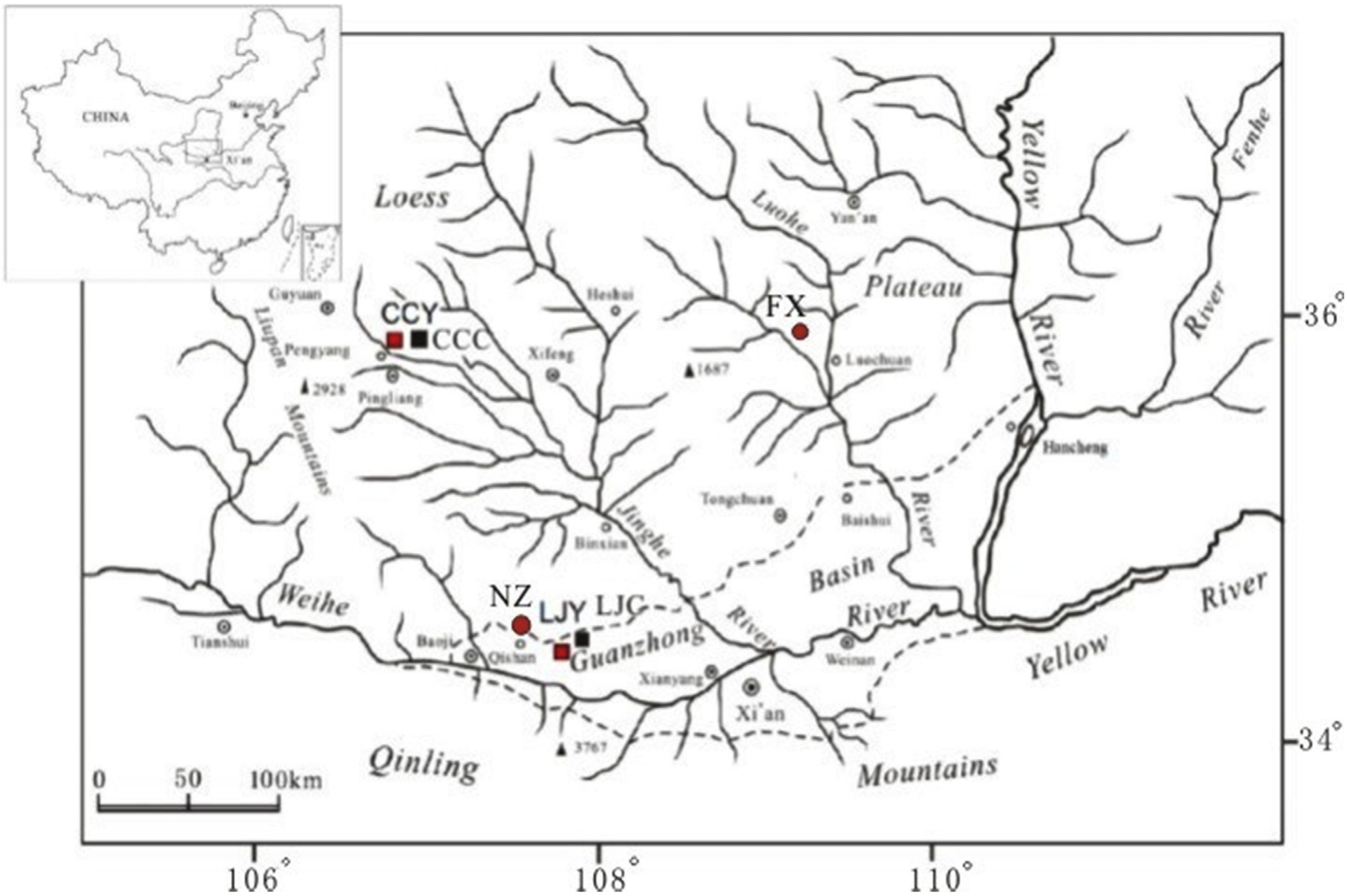

Fig. 1. Map showing the study region on the Loess Plateau. The study sites from black carbon and charcoal records are marked as boxes: Liangjiacun (LJC) site, Liangjiayao site (LJY, a previously-investigated site, Tan et al., 2015), and Nanguanzhang (NZ) site (Han, 2000) in the southern part of the Loess Plateau; Changchengchun (CCC)site, Changchengyuan site (CCY, a previously-investigated site, Tan et al., 2013)and Fuxian (FX) site (Cheng, 2011)in the northern part of the Loess Plateau; The pollen data used in the study sites from NZ and FX sites marked as circles.

Meanwhile, the vegetation composition and distribution of fire were greatly modified to human land farming on the Loess Plateau by the "slash and burn" method during the last thousand years (Huang et al., 2006; Tan et al., 2011).

The studies of wildfire history have rapidly developed during the past few decades. Currently, wildfire regimes were investigated throughout the world using biological geochemistry, remote sensing technology, atmospheric physics, environment modeling and other multi-disciplinary technologies (Kehrwald et al., 2013; Marlon et al., 2013). These studies greatly contribute to our understanding of the interaction between fire, vegetation and climate during Holocene. A key research focus initial is to understand the behavior of natural wildfires using historical database from remote sensing and tree ring studies (for the last fifty years only) or reports provided by governmental forestry departments from anthropogenic and natural ignitions (Kehrwald et al., 2013). Subsequently, an alternative source of evidence concerns fire regimes and its forcing driver from the reconstruction of past wildfire sequence, and also the study of wildfire history was from site-specific locations to establish intra- and inter-regional wildfire database (Haberle and Ledru, 2001; Huber et al., 2004; Higuera et al., 2007; Whitlock et al., 2007; Vanni'ere et al., 2008; Jiang et al., 2008; Marlon et al., 2009; Kaal et al., 2011; Han et al., 2012; X Wang et al., 2012). Recently, compilations of such records have produced useful global and regional syntheses of lateglacial to Holocene fire regimes from the Global Charcoal Database (Power et al., 2008; Daniau et al., 2012; Marlon et al., 2013). Most of their studies primarily focused on the correlation with fire and climate change at various scales, whereas few reports investigated the complex interaction between fire, and vegetation (fuel), climate and human activities.(Yang et al., 2001; X Wang et al., 2005; Huang et al., 2006; Zhou et al., 2007; Li et al., 2009; Tan et al., 2015; Miao et al., 2016a). Paleoecological research has shown that vegetation strongly mediates climate–fire relationship by altering landscape patterns of vegetation and fuels (Higuera et al., 2009). The occurrence and propagation of fires are strongly governed by the moisture content of the low fuel and sufficient high fuel accumulation. Recent studies show that wildfires could have occurred in relatively warm and dry climatic conditions during the early of Middle Holocene, whereas wildfire frequency was also an increase in cold and dry climatic conditions during the Late Holocene. This suggests that fuel characteristics also may be an important control rather than directly climate-determined influences on fire regimes in the semi-arid and sub-humid region (Christensen, 1993). However, there is no standard protocol attached to the charcoal and black carbon analysis from continental or marine sediment due to differences of regional scale. It is so difficult to establish comparisons between different paleo-environments throughout the world that a detailed understanding of the relations between fires, vegetation composition and climate change during the Holocene remains limited (Hawthorne et al., 2017; Tan et al., 2015; X Wang et al., 2013). Furthermore, there is no clear relation between fires, vegetation composition (C_3/C_4) and the distribution of human land use in response to the East Asian monsoon. We addressed this problem by investigating the interaction between wildfire, seasonal climate change and vegetation composition, as well as human land use at centennial-to-millennial time scales. The available charcoal and black carbon records will provide us an opportunity to examine the linkages with fire regime, the vegetation dynamics and human land use in response to the East Asian monsoon over the Loess Plateau.

2. Regional setting and loess profiles

The study sites include the Changchengcun (CCC) profile in the northern part of the loess tableland (35°52′0.8″N Lat.,106°46′43.9″E Long.; 1400 m a.s.l.) and the Liangjiacun (LJC) profile in the Guanzhong Basin in the south (34°26′46″N Lat., 107°40′27″E Long.; 640 m a.s.l.)The two investigated sites are aligned along a north–south transect across the Loess Plateau and span the gradient change of climates and vegetation types from a steppe to a forest-steppe landscape. The recorded mean annual temperature varies from 7.8 °C to 13.5 °C and the mean annual precipitation from 550 mm to 700 mm with 60% of the precipitation falling during July and September. The annual average evaporation ranges from 700 mm to 1200 mm (Qian, 1991, Fig. 1). The climate of the studied region is warmer and wetter during summer because the western Pacific subtropical high affects the southeast monsoon pattern, whereas a colder and more arid climate prevails during winter due to the impact of the northwest monsoon dominated by a high atmospheric pressure system coming from Inner Mongolia. This region is also the ecotone between Chinese traditional dry farming and nomadic pastoral practices. Here, wildfire activity has been highly susceptible to global and regional climate change and human land use since the Holocene. Meanwhile, the regional landscape has also experienced a long history of dry farming by means of the ignited fire method (“slash and burn”), which has been traced back to at least in past 8kyr (Li et al., 2009; Huang et al., 2004, 2006; 2009a; b; Archaeological Institute of CASS, 1991; Editorial Board, 1998). Many Neolithic settlements have since arisen on the Loess Plateau during the Holocene, such as the Laoguantai Culture (7.8–7.0kyrBP) and the Yangshao Neolithic Culture (7.0–5.5kyrBP; Tan et al., 2015). The profiles at the CCC site and a further site at Changchengyuan (CCY, a previous study site; Tan et al., 2013) are located in the northern part of Loess Plateau in the east of the Liupan Mountains and is on the margin of The Great Wall of China (Fig. 1). A total of 50 and 125 loess sediment samples were taken every 5 cm and 2 cm spaced continuously down the study profiles from ground surface at the CCY and CCC sites, respectively; the profiles at the LJC site and a further site at the Langjiayao (LJY; previously-investigated site, Tan et al., 2015) are situated on the southern part of the Loess Plateau (Guanzhong Basin). A total of 60 and 75 loess sediment samples were taken every 5 cm spaced continuously down the study profiles from ground surface at the LJY and LJC sites, respectively. Both sites are currently dominated by cultivated farming landscapes.

3. Stratigraphy and chronology

The loess stratigraphic sections and the robust OSL-derived chronology (optically stimulated luminescence) of the CCY and LJY profiles helped establish pedo-stratigraphic subdivisions principally defined by detailed observation of the color, texture and structure of the sediments in the fields (Archaeological Institute of CASS, 1991). The LJC and LJY profiles are situated on a flat or shallow saucer-shaped landscape in the western Guanzhong Basin. The two profiles are only separated by 100 m on the southern part of loess tableland (Fig. 1). Similarly, the CCC and CCY profiles, closely separated by 50 m, are located on the loess tableland in the northern part of Loess Plateau (Fig. 1). A Chernozem soil (Heilusol in Chinese, Chernozem in WRB) is developed in the steppe and observed at the CCY and CCC sites, while a Cinnamon soil (the Ustic Isohumisol) developed in the steppe-forest at the LJY and LJC sites, deposited in the southern part during the Middle Holocene (Tan et al., 2013). They are well preserved and the pedo-stratigraphy well-correlated in their stratigraphic sections (Figs. 1 and 2), and also share similar chronology, lithology, and vegetation types between them (Tan et al., 2013, 2015). The OSL age data determined from the profiles of the LJY and the CCY sites, integrated with the identification of archaeological remains and stratigraphic correlations, provides two reliable chronological framework, respectively (Fig. 3; Archaeological Institute of CASS, 1991; Gansu Museum, 1960; Huang et al., 2006; Tan et al., 2013). The chronological framework established in the study sites is well correlated with the other dating profiles over the Weihe River Drainage Basin (Fig. 2; Huang et al., 2003, 2004, 2009a; Tan et al., 2011, 2013,2015). The pedo-stratigraphic structure of the LJY and LJC profiles was described in detail by Tan et al. (2015). The CCY and CCC profiles is typical section of the Loess Plateau (Fig. 2). The pale yellowish-orange, silty, friable, porous and carbonate rich loess (L_1), the boundary between the Malan Loess (L_1) of the last glaciation and the Early Holocene transitional loess (L_t) were observed at depths of 190 cm and 180 cm for the CCY and CCC profiles, respectively. An OSL date of 11,490 ± 940yr was determined at a depth range of 185–180 cm in the CCY profile. This boundary is one of the most important stratigraphic markers of the Chinese loess-paleosol sequence, indicating the end of the last glacial period and the beginning of the Holocene at 11.5kyrBP (Roberts, 1992; Mayewski et al., 2004; Hoek and Bos, 2007). The slightly weathered or pedogenically modified Early Holocene transitional loess (L_t) was identified at depth intervals of 190–150 cm and 180–150 cm from the CCY and CCC profiles, respectively. The Ustic Isohumisol (S_0) was recognized at a depth range of 150–54 cm in the CCY and CCC profiles. An OSL date of 6740 ± 720yrBP was obtained from a depth range of 135–130 cm in the CCY profile. The paleosol (S_0) is widely distributed over the Loess Plateau and was dated at 8.5–3.1kyrBP (Huang et al., 2000). The Paleosol (S_0) is underlain by the transitional loess (L_t) of the early Holocene, and it is buried by the recent loess and the topsoil (L_0, TS) of the late Holocene age in the depth range of 54–0 cm in the CCY and CCC profiles. An OSL date of 2830 ± 400 yrBP was obtained at a depth of 60–55 cm in the top part of the recent loess in the CCY profile. The loess (L_0) is the most widely distributed and easily identifiable pedo-stratigraphic marker of the Holocene loess-paleosol profiles in the middle reaches of the Yellow River (Liu, 1988). Here, the recent loess (L_0) and topsoil (TS) layer of the late Holocene were identified above the depths of 20 cm in the profiles.

4. Methods

Magnetic susceptibility was measured with a Bartington MS_2 Magnetic Susceptibility Meter (0.47/4.7 kHz). The black carbon concentration was determined at the Key Laboratory of Aerosol Science and Technology on a DRI Model 2001Thermal/Optical Carbon Analyzer by thermal/optical reflectance (TOR) method as specified by the IMPROVE protocol (Han et al., 2007, 2009). The charcoal data used in this study was from the LJY and CCY profiles (Tan et al., 2013). The charcoal content was determined by thin section counting following the procedure described by Tan et al. (2013). The statistics for charcoal were analyzed and counted to obtain counts of fine particles (< 25μm), and coarse particles (> 100 μm) and to convert these to charcoal concentrations (grains/cm^2). The pollen data used in the study sites from the NZ (Nanguanzhang) site (Han,2000) and the Fuxian (FX) site (Cheng, 2011). The LJC and NZ sites share a similar climate and plant community in the southern part of loess tableland, whereas the CCC and FX sites share a similar climate and plant community in the northern part of loess tableland, although they are not from the same section.

The black carbon (EC-char and EC-soot) influx (mg C/cm^2per yr) and macro/micro-charcoal influx (grain/cm^2 per yr) were calculated by multiplying the black carbon (EC-char and EC-soot; mg/cm^3) and charcoal (macro-charcoal > 100 μm and micro-charcoal < 25 μm; grain/cm^3) concentrations by the sedimentation rate (cm/yr), following the decomposition technique of Long et al. (1998). The black carbon and macro/micro-charcoal influx of time series were then interpolated to constitute pseudo-annual accumulation rates and binned in 50yr time intervals. The binned concentration values were then divided by the average deposition times of each binned interval to obtain a time

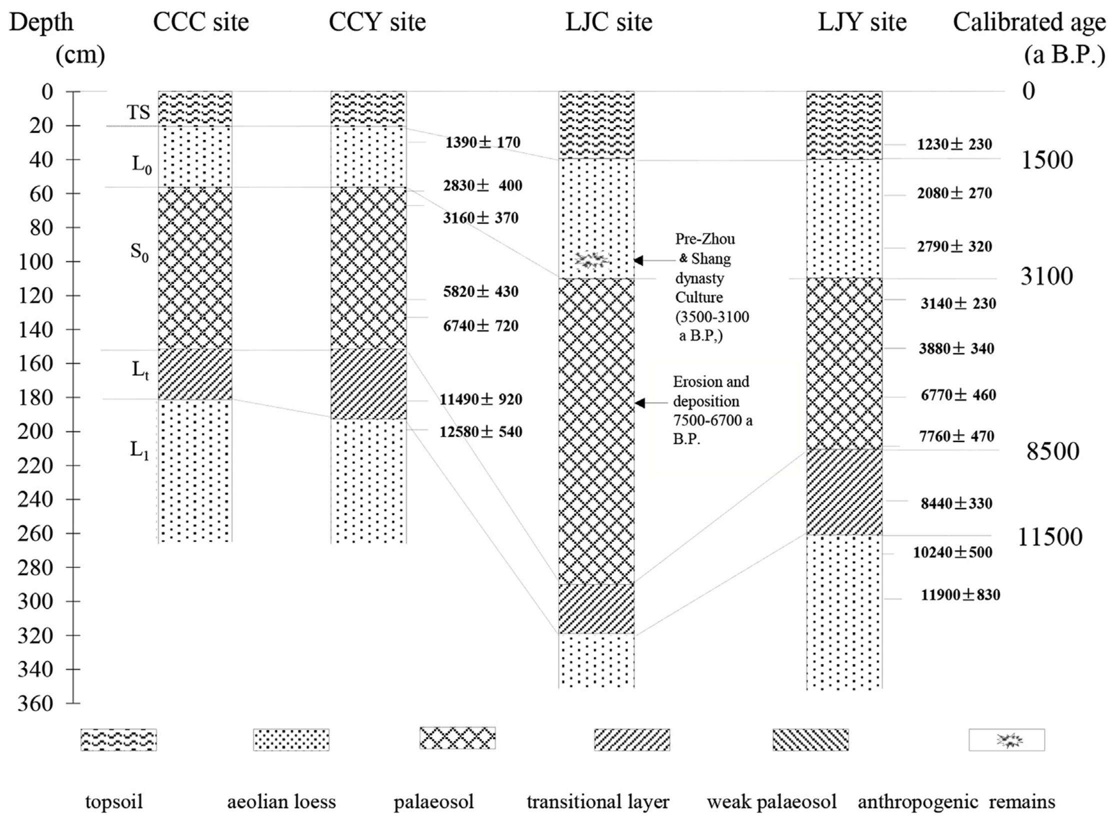

Fig. 2. Stratigraphic subdivision and chronology in the LJC profiles, LJY profiles, CCY profile and CCC profile over the Loess Plateau.

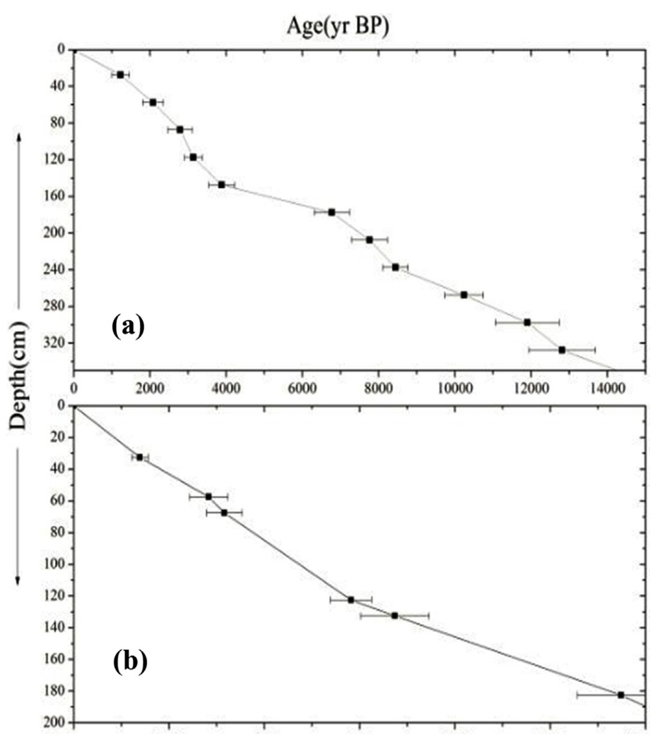

Fig. 3. Pedo-stratigraphic subdivision and the age/depth curve of the LJC profile (a) and the CCC profile (b) over the Loess Plateau.

series of charcoal accumulation rates (grains/cm^2 per. yr; Whitlock and Larsen,2001; Patterson et al., 1987).

The carbon isotopic composition was determined on a Finnigan-MAT-251 isotope ratio mass spectrometer located at the State Key Laboratory of Loess and Quaternary Geology, Chinese Academy of Sciences. The mass spectrometer uses a dual inlet system and a CS-344 elemental analyzer with a precision of ± 0.1‰. The C isotopic ratios were normalized to the PDB standard with a precision of < 0.2‰ or better (Liu et al., 2011). The relative abundance of C_4 plants as a percentage of the total vegetation biomass can be estimated through the equations elaborated by Vidic and Montañez (2004) specifically provided for the Loess Plateau, such as % C_4 = 100 × (27 + δ^{13}C)/14; where the average carbon isotope value of C_3 plants is −27‰ and that of C_4 plants is −14‰.

5. Results and interpretation

The magnetic susceptibility is one of the most important proxy in climate studies from Chinese loess-paleosol sequences (Maher et al., 1998; Huang et al., 2006). It records the changes in intensity of pedogenesis during dust accumulation, resulting from precipitation change connected with monsoonal climatic variation over Loess Plateau. (Maher, 1998; Maher and Alekseev, 2002; Balsam et al., 2004; An et al., 2000). The Magnetic susceptibility values also exhibit similar trends in corresponding with the layer of loess-paleosol profile at LJC and CCC sites. The values range from 52.5 × 10^{-8} to 251 × 10^{-8} m^3 kg^{-1}at the LJC site, showing a gradual increase from the Early to Late Holocene, followed by a gradual decrease to the present. The higher values suggest relatively concentrated ultra-fine-grained ferromagnetic minerals from pedogenesis during the Holocene Climatic Optimum, While lower values indicated climate aridity and intensified human disturbance by arable cultivation in the past 3kyrBP (Fig. 6). At the CCC site, the Magnetic susceptibility values vary from 36.2 × 10^{-8} to 83.4 × 10^{-8} m^3 kg^{-1}, showing a gradual increase from the Early Holocene to their highest values around 5.6kyrBP, followed by a gradual decrease to the present. The higher values also suggest a strong pedogenesis process during the Holocene Climatic Optimum. The sharp decrease below 70 × 10^{-8} m^3 kg^{-1}observed in the past 3kyr may be

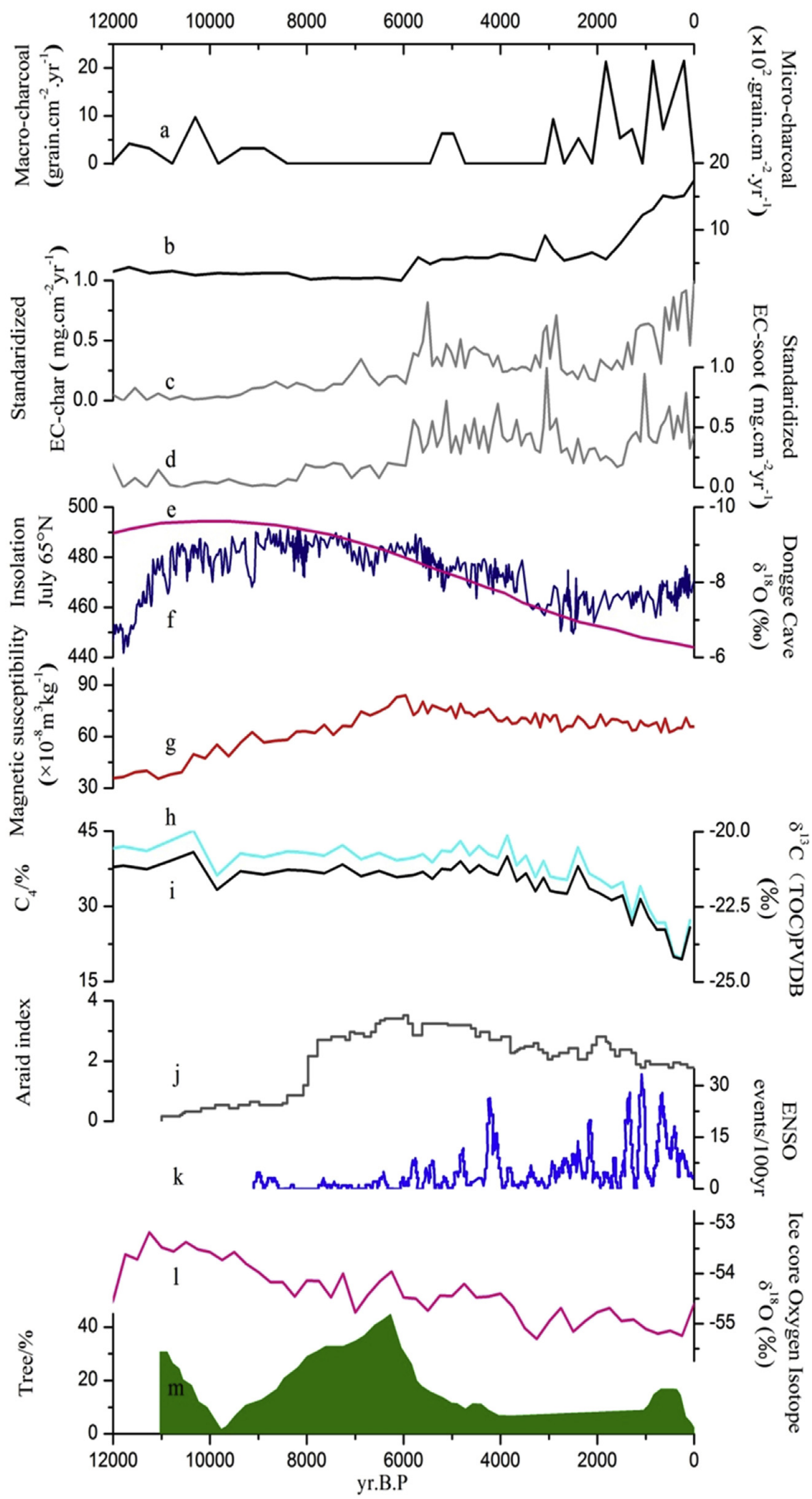

Fig. 4. Comparison of various proxies in the northern part of the Loess Plateau with other records during the last 12 ka; (*a*) macro-charcoal influx (> 100 μm) at the Changchengyuan (CCY) site (Tan et al., 2013); (*b*) micro-charcoal influx (< 25 μm) at the CCY site (Tan et al., 2013); (*c*) standardized EC-char influx values at the Changchengchen (CCC) site; (*d*) standardized EC-soot influx values at the CCC site; (*e*) July 65°N isolation is marked by a red line (Berger and Loutre, 1991); (*f*) $\delta^{18}O$ data from Dongge Cave (Dykoski et al., 2005) indicating regional moisture variations; (*g*) low-frequency of magnetic susceptibility data at the CCC site; (*h*) Composition of C_3 and C_4; (*i*) value of $\delta^{13}C$ of soil organic matter data at the CCC site; (*j*) The variation of moisture in the arid region of China (Chen F, 2008); (*k*). The number of events in ENSO variability during the Holocene (100-yr windows; Moy et al., 2002) (*l*) $\delta^{18}O$ data from the Dome Fuji Ice core (Kawamura et al., 2007) indicating the change of temperature in the northern hemisphere; (*m*) the percentage of tree pollen from the northern part of the Loess Plateau (Cheng, 2011). (For interpretation of the references to color in this figure legend, the reader is referred to the Web version of this article.)

related to farming (Fig. 4). Moreover, LJC and CCC at the two sites display obvious differences in moisture content and in the intensity of pedogenesis, implying steep climatic gradients from the northern to the southern part of the Loess Plateau.

Soil organic matter and pedogenic carbonate in sediments have been widely used to reconstruct the proportion of plants using C_3/C_4 photosynthetic pathways, and to identify the intensity of pedogenesis which was closely linked with the East Asian monsoon climate varibility (Cerling, 1984; O'Leary et al., 1988; Cerling et al., 1989; Quade et al., 1989, 1995; Ehleringer and Cerling, 2002).

During the Holocene, the $\delta^{13}C$ values of soil-derived organic matter ranges from −18‰ to −24‰ at the LJC site and from-21‰ to −24‰ at the CCC site (Fig. 5). The $\delta^{13}C$-based estimates of the abundance of C_4 plants for the entire Holocene averaged from 60% to 30% at LJC site and from 45% to 17.5% at CCC site, respectively. The differences in C_4 abundance between the two sites happened before 4kyrBP. The $\delta^{13}C$-

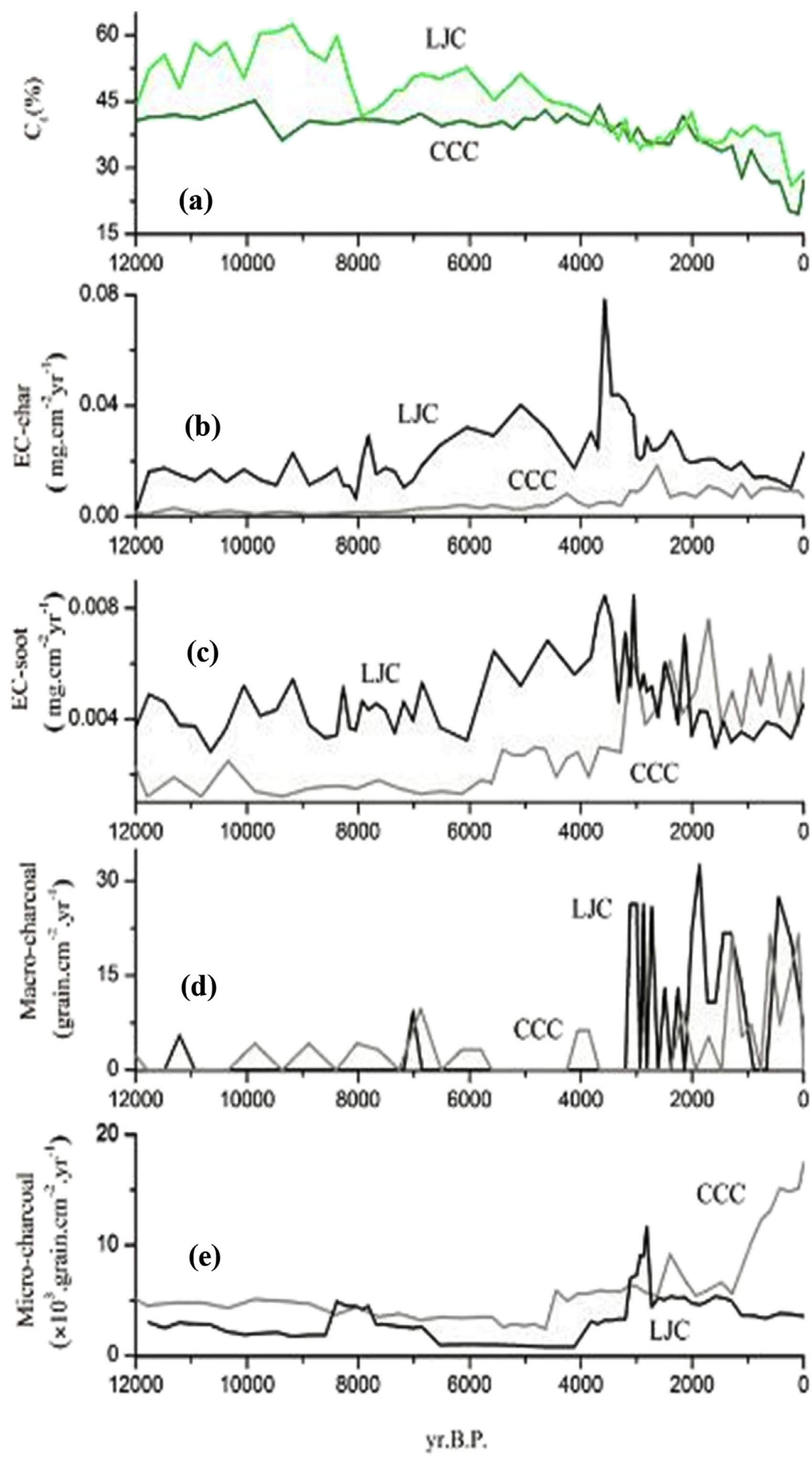

Fig. 5. Comparison of C_4 abundance (*a*), EC-char influx (*b*), EC-soot influx*(c)*, Macro-charcoal influx*(d)* and Micro-charcoal influx(*e*) at LJC (dark color curve) and CCC(light color curve) during the Holocene. (For interpretation of the references to color in this figure legend, the reader is referred to the Web version of this article.)

based estimates of C_4 plant abundance at the LJC site ranges from 60% to 30% with a general decreasing trend from the Early to Late Holocene (Fig. 5). The C_4 abundance at the CCC site varies from 45% to 15% and, unlike LJC, displays no significant trend from the Early to Late Holocene. However, the CCC site manifests larger fluctuations in C_4 abundance during the Late Holocene relative to the Early Holocene. Furthermore, the changes of $\delta^{13}C$ values of soil-derived organic matter at the LJC site are more obvious that of the CCC site, suggesting the climate was even colder and drier and in favor of C_3 plants growth at the CCC site than that of at the LJC site during the Late Holocene (Fig. 5).

The Micro-and Macro-charcoal influx differ between the LJY and CCY sites (Fig. 5). At LJY, the Micro-charcoal influx values range from 0.8 to 11.8 × 10^3particles of charcoal cm^{-2}yr^{-1}with maxima present during the Early Holocene, followed by a sharp decrease between 8.4 and 4.1kyrBP, and the strongest growth after 3.1kyrBP. The Micro-charcoal influx highest peaks occurring between 3.1 and 1.5kyrBP and 9–8kyrBP suggest an augmentation in regional fires and an increased amount of biomass during the Early and Late Holocene. On the other hand, Peak values of the macro-charcoal influx occur after 3.1kyrBP indicating local fires were infrequent near the study site until the Late Holocene.

At CCY, the Micro-charcoal influx values vary from 2.5 to 17.7×10^3grains. $cm^{-2}yr^{-1}$ and generally increase after the Middle Holocene, with the maximum increase beyond 1.5kyrBP(Fig. 5). The increase in Micro-charcoal influx implies a growth in regional fires and in the amount of biomass during the Late Holocene (Fig. 5). Furthermore, Macro-charcoal influx peaks occurring after 2.9kyrBP indicate that local fires were infrequent near the study site until the Late Holocene. However, much higher Micro-charcoal influx at the CCY site relative to LJY site signify more frequent fires during Holocene (Fig. 5).

Comparison of the macro-charcoal influx between the two sites reveals a similar high frequency of fires corresponding to intensive land use by humans in the past 3kyr in the entire Loess Plateau. Whereas the inferred large difference from micro-charcoal influx between the two sites implies the difference in regional fire frequency and fire extent from northern to southern part of Loess Plateau during Holocene.

High resolution analysis of black carbon preserved in accretionary loess–soil profiles has reconstructed fire history and human activity in response to climate change (Wang et al., 2005). The LJC site presents variations in EC-char and EC-soot influxes from 0.003 to 0.078 and 0.003–0.008 mg $cm^{-2}yr^{-1}$,respectively.They present a gradual increase from the Early Holocene and reach high values between 4–3kyrBP followed by a sharp decrease to the present (Fig. 5). High peaks in BC influx around 3.5kyrBP suggest an increase in regional fires or in the amount of biomass during the Late Holocene.

EC-char and EC-soot influxes from the CCC site vary from 0.0006 mg $cm^{-2}yr^{-1}$to 0.0223 mg $cm^{-2}yr^{-1}$and 0.0012 mg $cm^{-2}yr^{-1}$to 0.0101 mg $cm^{-2}yr^{-1}$, respectively. We observe a gradual increase between 8kyr and 3kyrBP, succeeded by the largest increase around past 3kyr and then a decrease to stable levels by past 2kyr (Fig. 5). The BC influx growth indicates an increase in regional fires or in the amount of biomass during the late part of the Middle Holocene and the Late Holocene (Fig. 5). In addition, the much lower BC influx at the CCC site relative to LJY during the Holocene reveals the burning of regional biomass being closely related to different build-up and composition of burnable biomass. However, since past 3kyr, the Soot Influx at the CCC site is higher than that of at LJY, signaling a more arid climate in the northern part of the studied region.

6. Discussion and conclusions

6.1. Fire, charcoal, and BC(char, soot)

The history of fires determined by Macro/micro-charcoal and BC(EC-soot and EC-char) records at the LJC and CCC sites demonstrate a roughly similar pattern of fluctuations during Holocene, consistently reflecting the regional emission of smoke carbonaceous particulate material and biomass burning activity (Thevenon et al., 2010). Both of the two sites present a transition in low amplitude peaks with a generally increasing trend during the early and middle of Holocene (11k-3kBPyr), while higher amplitude fire occurred during the Late Holocene (3kBPyr-0, Fig. 5). However, in the macro- and micro-charcoal record, the peaks in the two profiles occur primarily in the past 3kyrBP., whereas the highest values of BC (EC-soot and EC-char) influx still present frequently of 4-3kyrBP. (Fig. 5). The BC and charcoal records from Lake Daihai, about 1000 km to the northeast of the LJC site, shows the similar trends with the higher values (Han et al., 2012; Tan et al., 2015). The differences in the timing of the trends may be ascribed to either differences in fire history at spatial scales, or they may reflect differences in transportation mechanisms and fuel combustion efficiency (Thevenon et al., 2010; Tan et al., 2015; Han et al., 2016). Several aspects of the records can be interpreted in the context of the data on climate changes and human activities (Tan et al., 2015). In contrast to the records of regional biomass burning at the LJC and CCC sites (Fig. 5), EC-char/EC-soot influx at the LJC site is much higher than that at CCC site, while micro-charcoal influx at the LJC site is still obviously lower than that at CCC site, suggesting that regional fires at the LJC site did not consume as much biomass relative to the CCC site. Soot influx at the two sites show that there was an arid trend over Loess Plateau since Holocene, and especially the arid trend on the northern was stronger than that of the southern in the past 3keyearsB.P. inferred by the lines of evidence from $\delta^{13}C$ of soil organic matter, the Dongge cave $\delta^{18}O$ values and Magnetic susceptibility in the Loess Plateau (Figs. 4 and 5). The differences in the values of BC and charcoal influx suggest that: firstly, regional fuel accumulation and biomass between the two sites were an gradient changing trend from a steppe in the northern part of Loess Plateau to a forest-steppe landscape in the Southern; Secondly, Herb biomass provides highly flammable fuel for grassland fires on Loess Plateau, which likely tended to be of frequent low intensity and low combustion efficiencies, injecting particles only into low atmospheric levels; this may have yielded a very limited black carbon flux and a large charcoal influx to the deposition site recorded by a high charcoal and low BC influx during the early and late of Holocene (Wang et al., 1999; Umbanhowar, 1996; Umbanhowar and Mcgrath, 1998; Pearl, 1999). Lastly, lower combustion efficiencies tend to favor smoldering fires which produce more charcoal than BC(Yokelson et al., 2011). Regionally, Micro/macro-charcoal influx and fire-episode occurrences indicated that local and regional fires were more frequent during arid conditions, where steppe occurred in the loess tableland region, than in the Guanzhong Basin to the south (forest-steppe) during the early and middle of Holocene (Figs. 4 and 5). This fire pattern may have been controlled by a relatively steep gradient of precipitation and regional fuel availability over the Loess Plateau, significantly decreasing from south to north under the influence with the strengthening of the Asian monsoon in the last 9kyr (An et al., 2000; Chen et al., 2008; Tan et al., 2013; Zhao et al., 2010; Zhao and Yu, 2012; Miao et al., 2016b). Therefore, the higher black carbon flux at LJY relative to the CCC site is the result of different biomass accumulations, vegetation composition and the intensive land use by humans during the Late Holocene (Figs. 4 and 5, Qu et al., 2010).

Additionally, the records from BC (EC-char and EC-soot) and charcoal suggest changes in seasonal climate in relation to short-term climatic events (Fig. 4a–d). The subsequent increase in fire-episode frequency between 4 and 2kyrB.P.was consistent with the climatic“deterioration” events (4.2–4.0kyrBP) under cooler and drier conditions in the late Holocene and also with changes in the spatial and temporal distributions of Neolithic burning practices, such as land reclamation and crop cultivation, during those periods (e.g., expansion of C_3 plants). Many lines of evidence from climatic proxies from China's monsoonal regions have identified an abrupt climatic event between 4.2 and 4.0kyrBP (Wang et al., 1999; Wu and Liu, 2004). Therefore, fire patterns at the two sites may be attributed to the fuel availability and fuel combustion efficiencies, as well as the mechanism of particle transportation and deposition at various spatial scales (Tan et al., 2015; Han et al., 2016).

6.2. Climate, vegetation C_3/C_4 abundance and fire

A pervious study shows that the effective moisture variability and fuel characteristics are also the important control of the fire occurrence during the Early and Late Holocene (Tan et al., 2013). However, as with climate changes, distinct differences existed in vegetation composition and structure between the two sites which may affect fire occurrence during the Holocene (Neslon et al., 2004). Successful spread of fires requires a combination of sufficiently low fuel moisture content and sufficiently high fuel accumulation and continuity (Christensen, 1993). Here, we combine vegetation composition, the C_3/C_4 abundance and

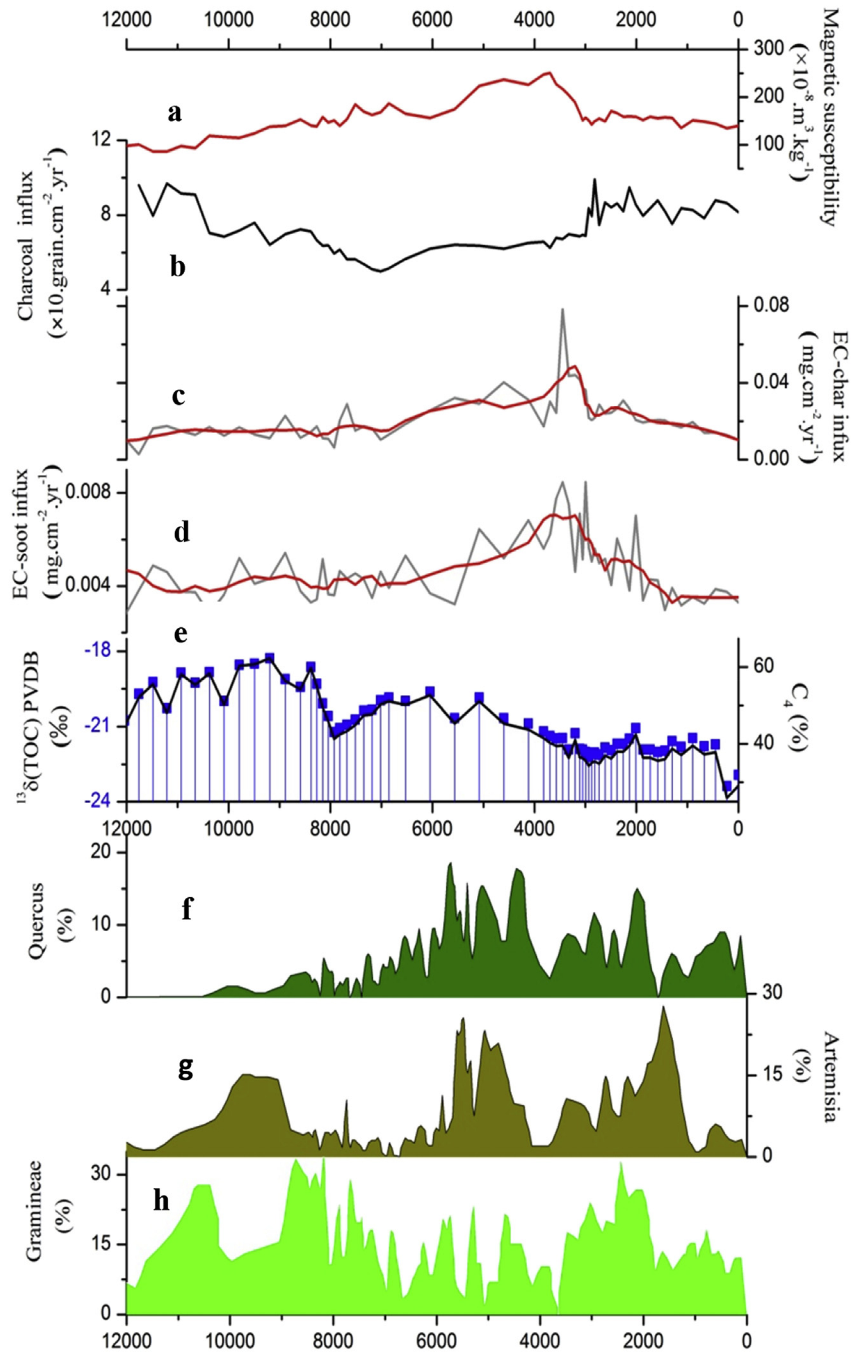

Fig. 6. Data used for climatic proxy (*a*, low-frequency of magnetic susceptibility), charcoal influx(*b*), EC-char influx(*c*),EC-soot influx(*d*), $\delta^{13}C$ (TOC) and the percent of C_4 (*e*), and *Quercus(f)*, *Artemisia(g)*, *Gramineae(h)* pollen abundance (Han, 2000) in the southern part of the Loess Plateau.

the frequency of fires from the two sites to discuss the trend of fire patterns at temporal and spatial scale in response to the East Asian monsoon climate.

The *Artemisia, Compositae,* and *Chenopodiaceae* pollens dominate a weedy C_3 taxon that includes herbs and shrubs along with a moderate abundance of *Gramineae* pollen (a weedy C_4 taxon) during the late glacial period. Their low concentration pollen presented at the NZ and FX sites suggests regional wildfires occasionally occurred on a highly disturbed and patchy desert steppe due to a lower effective moisture and limited fuel availability during those periods (Han, 2000; Cheng, 2011, Figs. 6 and 7). However, as with a climatic amelioration during the early of Holocene, the inferred C_4 plant-derived fires had an moderate increasing trend during those periods at the two sites. An increased C_4 (*Gramineae*)contribution to combusted biomass likely reflects an increase in source of fuel accumulation, presumably as a result of the conferring on C_4 taxa of a competitive advantage at interval of increased aridity, as inferred from the records of pollen and $\delta^{13}C$ of soil organic matter during those periods (Zhou et al., 2014; Han, 2000; Cheng, 2011).

The climate became warmer and drier (lower effective moisture variability)at the start of the Middle Holocene, inferred by the lines of evidence from $\delta^{13}C$ of soil organic matter, the Dongge cave $\delta^{18}O$ values and Magnetic susceptibility in the Loess Plateau (Fig. 4; Tan et al., 2015). The *Quercus* and *Artemisia* were 5% less abundant, along with *Gramineae* was 20% slightly abundant in pollen record at NZ sites; Whereas the *Corylus* and *Gramineae* were 5% less abundant, and *Artemisia* was more widespread at the FX site (Fig. 6). The pollen assemblage at both sites suggests fires rarely occurred on a arid steppe

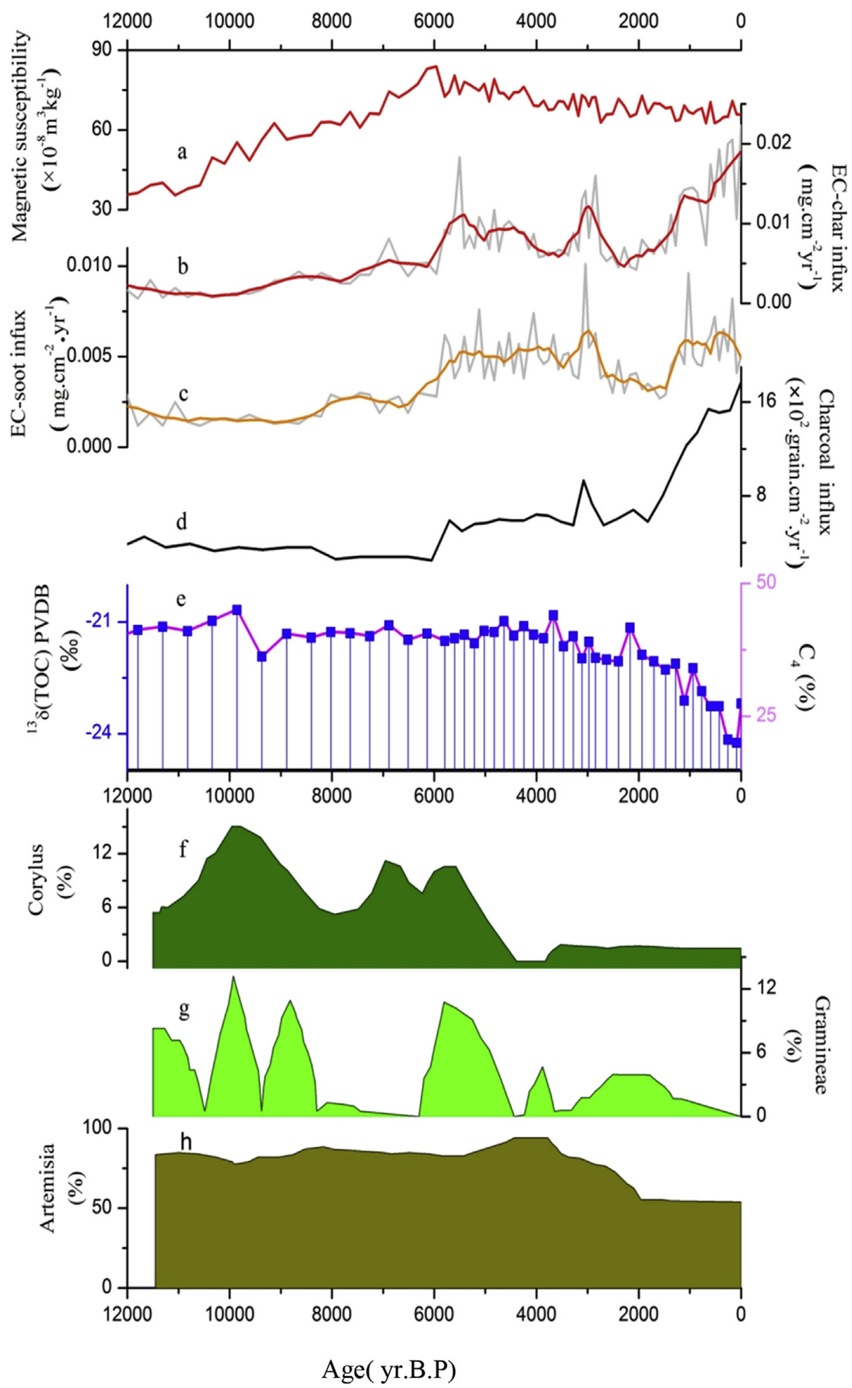

Fig. 7. Data used for climatic interpretation (*a*,low-frequency of magnetic susceptibility), EC-char influx(*b*),EC-soot influx(*c*), Charcoal influx (*d*), $\delta^{13}C$ (TOC) and the percent of C_4 (*e*), and *Corylus*(*f*), *Gramineae* (*g*), *Artemisia*(*h*) pollen abundance (Cheng, 2011) in the northern part of the Loess Plateau.

dominated C_3 plants of the loess plateau at the start of the Middle Holocene (Han, 2000; Cheng, 2011, Figs. 6 and 7). A reduced biomass (lower C_4 plant abundance) in an extremely arid and cold environment prevailing at 8.2kyrBP would have limited the propagation and the occurrence of fires (Han et al., 2012; Tan et al., 2015).

As the Holocene progressed with a warmer and wetter condition in the Middle of mid-Holocene recorded by the lines of evidence in the Loess Plateau (Figs. 6,7; Tan et al., 2015), the abundance and trees and shrubs pollen expanded substantially (an increasing of C_3 wood plants) during those periods (Figs. 6 and 7), which produced suboptimal and microclimatic conditions for C_4 taxa (Ehleringer et al., 1997). Whereas fire occurrence was reduced in the a forest-steppe of Loess plateau. Specifically, *Quercus* and *Artemisia* pollens increased in abundance from 5% to 20%, along with the *Gramineae* pollen decreased from 30% to 15% at the NZ site (Fig. 6);*Corylus* and *Gramineae* pollens increased in abundance from 6% to 12% and from 3% to 12%,respectively, While *Artemisia* showed an substain and little change at 70% at the FX site (Fig. 7) during the middle of Mid-Holocene. The abundance of the *Quercus* and *Artemisia* pollens declined from 15% to 6% during the end of the Middle Holocene with *Gramineae* showing a slight growth ranging from 15% to 30% at NZ site (Fig. 6). The FX site abundance of *Corylus* and *Gramineae* pollens fell from 12% to 3%, along with *Artemisia* showed a slight increase varying between 75% and 80% (Fig. 7).

During the Late Holocene, the climate became more arid and colder, coinciding with a climate aridity in the past 3kyr.The *Gramineae* and *Artemisia* abundance gradually decreased from 30% to 5% with an obvious diminution past 2kyr. The *Quercus* abundance decreased slightly between 12% and 5% during that period, while the inferred fire events gradually increased in the past 3kyr, followed by a diminution past 2 kyr at NZ site (Fig. 6). The FX, *Corylus* and *Gramineae* pollen abundance goes down below 5%. *Artemisia* gradually decreases from 80% to 60%, whereas the inferred fires occurrence increased past 2kyr (Fig. 7).

In short, the C_4 plants were more favor to competitive advantage than the C_3 plants during the interval of increased aridity between them, as inferred from records of pollen and $\delta^{13}C$ of soil organic matter influx, which likely provided more fuel sources for fire occurrence. On the other hand, the results presented here highlight the important role played by fire in a rise to prominence of C_4 taxa in semiarid steppe grassland on Loess Plateau since the early Holocene, along with increasing aridity and seasonality. As can more easily occur fires in the eastern part of Inner Mongolia in China than that of the western every spring in the last five years, which the limited distribution of C_3 plants could not meet fires spread in the extreme dry climate condition (Li et al., 2004).

6.3. Fire and human land use in response to climatic change

The application of paleo-fires is one of the earliest ecological management tools by human (Bowman et al., 2009). Apparently, asynchronous fire patterns appear to be the close links with regional and temporal variations and intensities of human activity during the onset of a drier climate in the region during the late Holocene (Tan et al., 2013). Specifically, Historical documents recorded that as the Holocene progressed towards a colder and drier climate, the ancestors of the Pre-Dynasty Zhou tribes who lived in the arid northern part of Loess Plateau had migrated to the Guanzhong Basin (the southern part of Loess Plateau), resulting from the shortage of forage availability and the north tribes invasion during 3kyrBP.Subsequently, an evident increase in charcoal and BC influx indicate biomass burning to reclaim land for cereal cultivation increased to an unprecedented scale over the southern part of the study region during those periods. Whereas the gradual increase in both C_4 (Gramineae) taxa and charcoal influx around 3kyr BP and subsequent a decrease in the stable level indicate human beings thus apparently were largely responsible for semi-arid ecological landscape evolution. Archaeological and paleoecological records show that a number of settlements were built at this time and handicraft and bronze industries developed as observed in the Qishan county (Huang et al., 2009b; Tan et al., 2015; Archaeological Institute of CASS, 1991). Therefore, it can be inferred that primeval forest-steppe landscape has been gradually replaced by the agricultural landscape in the study area formed by deliberate burning means of wildfire in the southern part of the study region since 3kyr BP (Huang et al., 2006; Tan et al., 2011). In contrast, an obvious increase in charcoal and BC influx indicate biomass burning to reclaim land for cereal cultivation increased to a higher level over the northern part of the study region till 2kyrB.P. Archaeological records indicate that an increasing number of migrants poured in at the time and much more land was reclaimed for dry farming in the north, when the Great Wall was under construction on the northern part of loess tableland in order to defend against the invasion from the north tribes during the Qin-Han Dynasty periods (2170–1730yrBP).(Huang et al., 2006, 2009b; Archaeological Institute of CASS, 1991). This result was confirmed by the remains of settlement during the Qin and Han Dynasties which was found in the study site nearby (Archaeological Institute of CASS, 1991; Huang et al., 2009b). Meanwhile, the gradual increase in both C_4 pollen (Gramineae) and microscopic charcoal since about 2kyrB.P. and a sharp decrease in C_4 taxa (Gramineae) but an increase in micro-charcoal influx at 1.5kyr BP suggest that all the land suitable for farming had been reclaimed and replaced by the farming system of terraced fields and dry farming landscapes was gradually established in the northern part of the study region around 1.5kyr BP (Tan et al., 2008; 2013). However, high charcoal and BC influx in the present plowed layer at the CCY profile perhaps arise from the burning of wheat and maize stalks in fields since1.5kyr BP (Huang et al., 2006; Tan et al., 2013).

Heterogeneous fire patterns across the Loess Plateau reveal the interaction between fire regime, ecological landscape and the regional and temporal distribution of human land use in response to East Asian monsoon climate change over the long term (Marlon et al., 2013).

Acknowledgements

We thank Prof. Boris and Prof. Mitchell J Power for their inviting us to make a contribution. This research was sponsored by grants from Natural Science Foundation of China (No.41771218; No.41271228; 41625015; 41473119); the Chinese Academy of Sciences (QYZDY-SSW-DQC001 and ZDBS-SSW-DQC001), the MOST (2016YFE0109500), the Open Fund of State Key Laboratory of Loess and Quaternary Geology, Institute of Earth Environment, CAS (No.SKLLQG1518; No.SKLLQG1618); and the Open Fund of Key Laboratory of Aerosol Chemistry and Physics, Institute of Earth Environment, CAS (No.KLACP141201). Special thanks should also go to those who work anonymously to make this collaboration a complete success.

References

An, Z.S., Porter, S., Kutzbach, J.E., Wu, X.H., Wang, S.M., Liu, X.D., Li, X.Q., Zhou, W.J., 2000. Asynchronous Holocene optimum of the east Asian monsoon. Quat. Sci. Rev. 19, 743–762.

Archibald, S., Roy, D.P., van Wilgen, B.,W., Scholes, R.,J., 2008. What limits fire? An examination of drivers of burnt area in Southern Africa. Glob. Change Biol. 15 (3), 613–630.

Balsam, W., Ji, J., Chen, J., 2004. Climatic interpretation of the Luochuan and Lingtai loess sections, China, based on changing iron oxide mineralogy and magnetic susceptibility. Earth Planet. Sci. Lett. 223, 335–348.

Berger, A.M., Loutre, F., 1991. Insolation values for the climate of the last 10 million years. Quat. Sci. Rev. 10, 297–317.

Bowman, D.M.J.S., Balch, J.K., Artaxo, P., Bond, W.J., Carlson, J.M., Cochrane, M.A., D'Antonio, C.M., DeFries, R.S., Doyle, J.C., Harrison, S.P., Johnston, F.H., Keeley, J.E., Krawchuk, M.A., Kull, C.A., Marston, J.B., Moritz, M.A., Prentice, I.C., Roos, C.I., Scott, A.C., Swetnam, T.W., van der Werf, G.R., Pyne, S.J., 2009. Fire in the earth system. Science 324, 481–484.

Cerling, T.E., 1984. The stable isotopic composition of modern soil carbonate and its relationship to climate. Earth Planet. Sci. Lett. 71, 229–240.

Cerling, T.E., Quade, J., Wang, Y., Bowman, J.R., 1989. Carbon isotopes in soils and paleosol as ecology and paleoecology indicators. Nature 341, 138–139.

Chen, F.H., Yu, Z.C., Yang, M.L., Ito, E., Wang, S.M., Madsen, D.B., Huang, X.Z., Zhao, Y., Sato, T., Birks, H.J.B., Boomer, I., Chen, J.H., An, C.B., Wünnemann, B., 2008. Holocene moisture evolution in arid central Asia and its out-of-phase relationship with Asian monsoon history. Quat. Sci. Rev. 27, 351–364.

Cheng, Y.F., 2011. Vegetation and Climate Changes in the Middle and Northern Part of Loess Pateau over the Past 26000years. Master Dissertation. China University of Geosciences (in Chinese).

Christensen, N.L., 1993. Fire regimes and ecosystem dynamics. In: Crutzen, P.J., Goldammer, J.G. (Eds.), Fire in the Environment:The Ecological, Atmospheric, and Climatic Importance of Vegetation Fires. Wiley, Chichester, pp. 233–244 7. Background and Local Charcoal in Sediments: Scales of Fire Evidence in the Paleorecord. Sediment Records of Biomass Burning and Global Change 51, 23–48.

Conedera, M., Tinner, W., Neff, C., Meurer, M., Dickens, A.F., Krebs, P., 2009. Reconstructing past fire regimes: methods, applications, and relevance to fire management and conservation. Quat. Sci. Rev. 28, 555–576.

Daniau, A.L., Harrison, S.P., Bartlein, P.J., 2009. Fire regimes during the last glacial. Quat. Sci. Rev. 1–13.

Daniau, A.L., et al., 2012. Predictability of biomass burning in response to climate changes. Glob. Biogeochem. Cycles 26 GB4007.

Dykoski, C.A., Edwards, R.L., Cheng, H., Yuan, D., Cai, Y., Zhang, M., Lin, Y., Qing, J., An, Z., Revenaugh, J., 2005. A high-resolution absolute-dated Holocene and deglacial Asian monsoon record from Dongge Cave, China. Earth Planet. Sci Lett. 233, 71–86.

Editorial Board, 1998. An Atlas of the Chinese Relics: Shaanxi Province. Xi'an Maps Press, Xi'an, pp. 1223 in Chinese.

Ehleringer, J.R., Cerling, T.E., 2002. C3 and C4 photosynthesis. In: In: Mooney, H.A., Canadell, J.G. (Eds.), The Earth System: Biological and Ecological Dimensions of Global Environmental Change: Encyclopedia of Global Environmental Change, vol. 2. John Wiley & Sons, Ltd, Chichester, pp. 186–190.

Ehleringer, J.R., Cerling, T.E., Helliker, B.R., 1997. C4 photosynthesis, atmospheric CO2, and climate. Oecologia 112, 285 er, B.R., 1997, C4 photosynthesis.

Haberle, S.G., Ledru, M.P., 2001. Correlations among charcoal records of fires from the past 16,000 Years in Indonesia, Papua New Guinea,and central and south America.

Quat. Res. 55, 97–104.
Han, Y.P., 2000. Holocene Vegetation and Environmental Change in Zhouyuan (Qishan) Region. Master Dissertation. Shaanxi Normal University (in Chinese).
Han, Y.M., Cao, J.J., Chow, J.C., Watson, J.G., Fung, K., Jin, Z.D., Liu, S.X., An, Z.S., 2007. Evaluation of the thermal/optical reflectance method for discrimination between char- and soot-EC. Chemosphere 69, 569–574.
Han, Y.M., Cao, J.J., Posmentier, E.S., Chow, J.C., Watson, J.G., Fung, K.K., Jin, Z.D., Liu, X., An, Z.S., 2009. The effect of acidification on the determination of elemental carbon, char-, and soot-elemental carbon in soils and sediments. Chemosphere 75, 92–99.
Han, Y.M., Marlon, J.R., Cao, J.J., Jin, Z.D., An, Z.S., 2012. Holocene linkages between char, soot, biomass burning and climate from Lake Daihai, China. Glob. Biogeochem. Chang. 26 (4) GB4017.
Han, Y.M., Peteet, D.M., Arimoto, R., Cao, J.J., An, Z.S., Sritrairat, S., Yan, B.Z., 2016. Climate and fuel controls on north American paleofires: smoldering to flaming in the late-glacial-holocene transition. Sci. Rep. 6, 20719. http://dx.doi.org/10.1038/srep20719.
Hawthorne, D., Mustaphiet, C.J.C., Aleman, J.C., Blarquezal, O., Colombaroli, D., Daniau, A.L., Marlon, J.R., Power, M., Vannière, B., Han, Y.M., Hantson, S., Kehrwald, N., Magi, B., Yue, X., Carcaillet, C., Marchant, R., Ogunkoya, A., Githumbi, E.N., Muriuki, R.M., 2017. Global Modern Charcoal Dataset (GMCD): a tool for exploring proxy-fire linkages and spatial patterns of biomass burning. Quat. Int. https://doi.org/10.1016/j.quaint.2017.03.046.
Higuera, P.E., Peters, M.E., Brubaker, L.B., Gavin, D.G., 2007. Understanding the origin and analysis of sediment charcoal records with a simulation model. Quat. Sci. Rev. 26, 1790–1809.
Higuera, P.E., Brubaker, L.B., Anderson, P.M., Hu, F.S., Brown, T.A., 2009. Vegetation mediated the impacts of postglacial climate change on fire regimes in the south-central Brooks Range, Alaska. Ecol. Monogr. 79 (2), 201–209.
Hoek, W.Z., Bos, J.A., 2007. Early Holocene climate oscillations—causes and consequences. Quat. Sci. Rev. 26, 1901–1906.
Huang, C.C., Su, H., 2009b. Climate change and Zhou relocations in early Chinese history. J. Hist. Geogr. 35, 297–310.
Huang, C.C., Zhou, J., Pang, J.L., 2000. A regional aridity phase and its possible cultural impact during the Holocene Megathermal in the Guanzhong Basin, China. Holocene 10 (1), 135–142.
Huang, C.C., Pang, J.L., Chen, S.E., Zhang, Z.P., 2003. Holocene dust accumulation and the formation of policyclic Cinnamon soils in the Chinese loess plateau. Earth Surf. Process. Landforms 28 (12), 1259–1270.
Huang, C.C., Pang, J.L., Zhou, Q.Y., et al., 2004. Holocene pedogenic change and the emergence and decline of rain-fed cereal agriculture on the Chinese loess plateau. Quat. Sci. Rev. 23 (23–24), 2529–2539.
Huang, C.C., Pang, J.L., Chen, S.E., Su, H., Han, J., Cao, Y., Zhao, W., Tan, Z.H., 2006. Charcoal records of fire history in the Holocene loess–soil sequences over the southern Loess Plateau of China. Palaeogeogr. Palaeoclimatol. Palaeoecol. 239, 28–44.
Huang, C.C., Pang, J., Su, H., Wang, L., Zhu, Y., 2009a. The ustic Isohumisol (Chernozem) distributed over the Chinese loess plateau: modern soil or palaeosol? Geoderma 150, 344–358.
Huber, U.M., Markgraf, V., Schabitz, F., 2004. Geographical and temporal trends in late Quaternary fires histories of Fuego-Patagonia, South America. Quat. Sci. Rev. 23, 1079–1097.
Institute of Archaeology, CASS, 1991. Collection of the ^{14}C Dates in Chinese Archaeology between 1965–1991. Cultural Relics Publishing House, Beijing, pp. 125–131 (in Chinese).
Jiang, W.Y., Leroy, S.A.G., Ogle, N., Chu, G.Q., Wang, L., Liu, J.Q., 2008. Natural and anthropogenic forest fires recorded in the Holocene pollen record from a Jin- chuan peat bog, northeastern China. Palaeogeogrphy. Palaeoclim. Palaeoecol. 261, 47–57.
Kaal, J., Marco, Y.C., Asouti, E., Seijo, M.M., Cortizas, A.M., Cas_ais, M.C., Boado, F.C., 2011. Long-term deforestation in NW Spain: linking the Holocene fire history to vegetation change and human activities. Quat. Sci. Rev. 30, 161–175.
Kawamura, K., Parrenin, F., Lisiecki, L., Uemura, R., Vimeux, F., Severinghaus, J.P., Hutterli, M.A., Nakazawa, T., Aoki, S., Jouzel, J., Raymo, M.E., Matsumoto, K., Nakata, H., Motoyama, H., Fujita, S., Goto-Azuma, K., Fujii, Y., Watanabe, O., 2007. Northern Hemisphere forcing of climatic cycles in Antarctica over the past 360,000 years. Nature 448, 912–916.
Kehrwald, N.M., Whitllock, C., Barbante, M.C., Max, V.B., Daniau, A.L., Kaplan, J.O., Marlon, J.R., Power, M.J., Thonicke, K., Werf, G.R., 2013. Fire research: linking past, present, and future data. EOS 94 (46), 421–432.
Li, X.H., Yang, L.P., Lv, D.B., 2004. The cause of Frost Fire occurrence and its forecast of fire risk on the inner Mongolian during summer. Meteorology J. Inn. Mong. 27 (2).
Li, X.Q., Shang, X., Dodson, J., Zhou, X.Y., 2009. Holocene agriculture in the Guanzhong Basin in NW China indicated by pollen and charcoal evidence. Holocene 19, 1213–1220.
Liu, T.S., 1988. Loess in China, second ed. Springer, Berlin, pp. 1–251.
Liu, W., Yang, H., Sun, Y., Wang, X., 2011. $\delta^{13}C$ Values of loess total carbonate: a sensitive proxy for Asian summer monsoon in arid northwestern margin of the Chinese loess plateau. Chem. Geol. 284, 317–322.
Long, C.J., Witlock, C., Bartlein, P.J., Millspaugh, S.H., 1998. A 9000-year fire history from the Oregon Coast Range, based on a high-resolution charcoal study. Can. J. For. Res. 28, 774–787.
Maher, B.A., 1998. Magnetic properties of modern soil and Quaternary loessic soils: palaeoclimatic implications. Palaeogeogr. Palaeoecol. 137, 25–54.
Maher, B.A., Alekseev, A.T., 2002. Variation of soil magnetism across the Russian steppe: its significance for use of soil magnetism as a palaeorainfall proxy. Quat. Sci. Rev. 21, 1571–1576.
Marlon, R.J., Bartlein, P., Walsh, M.K., Harrison, S.P., Brown, K.J., Edwards, M.E., Higuera, P.E., Power, M.J., Anderson, R.S., Briles, C., Brunelle, A., Carcaillet, C., Hu, F.S., Lavoie, M., Long, C., Minckley, T., Richard, P.J.H., Scott, A.C., Shafer, D.S., Tinner, W., Umbanhowar Jr., C.E., Whitlock, C., 2009. Wildfire responses to abrupt climate change in North America. PNAS 106, 2519–2524.
Marlon, R.J., Bartlein, P.J., Daniau, A.L., Harrison, S.P., Maezumi, S.Y., Power, M.J., Tinner, W., Vanni_ere, B., 2013. Global biomass burning: a synthesis and review of Holocene paleofire records and their controls. Quat. Sci. Rev. 65, 5–25.
Miao, Y., Jin, H., Cui, J., 2016a. Human activity accelerating the rapid desertification of the Mu Us sandy lands, north China. Sci. Rep. 6, 23003. http://dx.doi.org/10.1038/srep23003.
Miao, Y.F., Fang, X.M., Song, C.H., Yan, X.L., Zhang, P., Meng, Q.Q., Li, F., Wu, F.L., Yang, S.L., Kang, S.Y., Wang, Y.P., 2016b. Late Cenozoic fire enhancement response to aridification in mid-latitude Asia: evidence from microcharcoal records. Quat. Sci. Rev. 139, 53–66.
Moreira, F., Viedma, O., Arianoutsou, M., Curt, T., Koutsias, N., Rigolot, E., Barbati, A., Corona, P., Vaz, P., Xanthopoulos, G., Mouillot, F., Bilgili, E., 2011. Landscape-wildfire interactions in southern Europe:implications for landscape management. J. Environ. Manag. 92, 2389–2402.
Moy, C.M., Seltzer, G.O., Rodbell, D.T., Anderson, D.M., 2002. Variability of EI Nino/Southern oscillation acitivity at millennal timescales during the Holocene epoch. Nature 420 (6912), 162–167.
Gansu Museum, 1960. The ancient culture remains of Gansu. J. Archaeol. 2, 11–51 (in Chinese).
Nelson, D.M., Sheng, H.F., Tian, J., Stefanova, I., Brown, T.A., 2004. Response of C_3 and C_4 plants to middle-Holoceneclimatic variation near the prairie–forest ecotone of Minnesota. PNAS 101 (2), 562–567.
O'Leary, M.H., 1988. Carbon isotopes in photosynthesis. Bioscience 38, 328–336.
Patterson, W.A., Edwards, K.J., Maguire, D.J., 1987. Microscopic charcoal as a fossil indicator of fire. Quat. Sci. Rev. 6, 3–23.
Pearl, C.A., 1999. A Holocene Environmental History of the Willamette Valley, Oregon: Insights from an 11,000-year-record from Beaver lake. M.S. thesis. University of Oregon, Eugene, OR.
Pechony, O., Shindell, D.T., 2010. Driving forces of global wildfires over the past millennium and the forthcoming century. PNAS 107 (45), 19167–19170.
Power, M.J., Marlon, J., Ortiz, N., et al., 2008. Changes in fire activity since the Last Glacial Maximum: an assessment based on a global synthesis and analysis of charcoal data. Clim. Dyn. 3, 887–907.
Qian, L.O., 1991. Climate of the Loess Plateau. Meteorology Press, Beijing, pp. 369 (in Chinese).
Qu, Z.P., Zheng, S.X., Bai, Y.F., 2010. Geographical and temporal pattern in fire behaviors and their control. Chin. J. Appl. Ecol. 21 (4), 807–813.
Quade, J., Cerling, T.E., Bowman, J.R., 1989. Development of Asian monsoon revealed by marked ecological shift during the latest Miocene in northern Pakistan. Nature 342, 163–166.
Quade, J., Cater, J.M.L., Ojha, T.P., Adam, J., Harrison, T.M., 1995. Late Miocene environmental change in Nepal and the northern Indian subcontinent: stable isotopic evidence from paleosoil. Geol. Soc. Am. Bull. 107, 1381–1397.
Roberts, N., 1992. The Holocene: an Environmental History. Blackwell, Oxford, pp. 1–315.
Tan, L.C., An, Z.S., Cai, Y.J., Long, H., 2008. Hydrological representation of the 4.2kaBP event in China and its global linkages. Geol. Rev. 54, 94–104 (in Chinese with English abstract).
Tan, Z.H., Huang, C.C., Pang, J.L., Zhou, Q.Y., 2011. Holocene wildfires related to climate and land-use change over the Weihe River Basin, China. Quat. Int. 234, 167–173.
Tan, Z., Huang, C.C., Pang, J.L., Zhou, Y., 2013. Wildfire history and climatic change in the semi-arid loess tableland in the middle reaches of the Yellow River of China during the Holocene: evidence from charcoal records. Holocene 23 (10), 1466–1476.
Tan, Z.H., Han, Y.M., Cao, J.J., Huang, C.C., An, Z.S., 2015. Holocene wildfire history and human activity from high-resolution charcoal and elemental black carbon records in the Guanzhong Basin of the Loess Plateau, China. Quat. Sci. Rev. 109, 76–87.
Thevenon, F., Williamson, D., Bard, E., Anselmetti, F.S., Beaufort, L., Cachier, H., 2010. Combining charcoal and elemental black carbon analysis in sedimentary archives: implications for past fire regimes, the pyrogenic carbon cycle, and the human–climate interactions. Glob. Planet. Change 72, 381–389.
Umbanhowar Jr., C.E., 1996. Recent fire history of the northern Great Plains. Amer. Midl. Nat. 135, 115–121.
Umbanhowar Jr., C.E., Mcgrath, M.J., 1998. Experimental production analysis of microscopic charcoal from wood, leaves and grasses. Holocene 8 (3), 341–346.
Vanni'ere, B., Colombaroli, D., Chapron, E., Leroux, A., Tinner, W., Magny, M., 2008. Climate versus human-driven fire regimes in Mediterranean landscapes: the Holocene record of Lago dell'Accesa (Tuscany, Climate versus human-driven fire regimes in Mediterranean landscapes: the Holocene record of Lago dell'Accesa (Tuscany, Italy). Quat. Sci. Rev. 27, 1181–1196.
Vidic, N.J., Montañez, I.P., 2004. Climatically driven glacial–interglacial variations in C_3 and C_4 plant proportions on the Chinese Loess Plateau. Geology 32, 337–340.
Wang, L., Sarnthein, M., Erlenkeuser, H., Grootes, P.M., Grimalt, J.O., Pelejero, C., Linck, G., 1999. Holocene variations in Asian monsoon moisture: a bidecadal sediment record from the South China Sea. Geophys. Res. Lett. 26, 2889–2892.
Wang, X., Kaars, S., Kershaw, P., Bird, M., 1999. A record of fire, vegetation and climate through the last three glacial cycles from Lombok Ridge core G6–4, eastern Indian Ocean, Indonesia. Palaeogeogr. Palaeoclimatol. Palaeoecol. 147, 241–256.
Wang, X., Peng, P.A., Ding, Z.L., 2005. Black carbon records in Chinese Loess Plateau over the last two glacial cycles and implications for paleofires. Palaeogeogr. Palaeoclimatol. Palaeoecol. 223, 9–19.
Wang, X., Ding, Z.L., Peng, P.A., 2012. Changes in fire regimes on the Chinese Loess

Plateau since the last glacial maximum and implications for linkages to paleoclimate and past human activity. Palaeogeogr. Palaeoclimatol. Palaeoecol. 315–316, 61–74.

Wang, X., Xiao, J.L., Cui, L.L., Ding, Z.L., 2013. Holocene changes in fire frequency in the Daihai Lake region (north-central China): indications and implications for an important role of human activity. Quat. Sci. Rev. 59, 18–29.

Whitlock, C., Larsen, C.V., 2001. Charcoal as a fire proxy. Terrestrial, Algal, and Siliceous Indicators In: In: Smol, J.P., Birks, H.J.B., Last, W.M. (Eds.), Tracking Environmental Changes Using Lake Sediments, vol. 3 Kluwer Academic Publishers, Dordrecht 75pp.

Whitlock, C., Moreno, P.I., Bartlein, P., 2007. Climatic controls of Holocene fire patterns in southern South America. Quat. Res. 68, 28–36.

Wu, W.X., Liu, T.S., 2004. Possible role of the “Holocene event 3” on the collapse of neolithic cultures around the central plain of China. Quat. Int. 117, 153–166.

Yang, Y., Shen, C.D., Yi, W.X., Sun, Y.M., Liu, T.S., 2001. The elemental carbon record in Weinan loess section since last 21ka. Chin. Sci. Bull. 46, 1541–1544 (in Chinese with English abstract).

Yokelson, R.J., Burling, I.R., Urbanski, S.P., Atlas, E.L., Adachi, K., Buseck, P.R., Wiedinmyer, C., Akagi1, S.K., Toohey, D.W., Wold, C.E., 2011. Trace gas and particle emissions from open biomass burning in Mexico. Atmos. Chem. Phys. 11, 6787s. http://dx.doi.org/10.5194/acp-11-6787-2011. Chem.

Zhao, Y., Yu, Z., 2012. Vegetation response to Holocene climate change in East Asian monsoon-margin region. Earth-Science Rev. 113, 1–10.

Zhao, Y., Chen, F.,H., Zhou, A.F., Yu, Z.C., Zhang, K., 2010. Vegetation history, climate change and human activities over the last 6200 years on the Liupan Mountains in the southwestern Loess Plateau in central China. Palaeogeogr. Palaeoclimatol. Palaeoecol. 293, 197–205.

Zhou, B., Shen, C.D., Sun, W.D., Zheng, H.B., Yang, Y., Sun, Y.B., An, Z.S., 2007. Elemental carbon record of paleofire history on the Chinese Loess Plateau during the last 420 ka and its response to environmental and climate changes. Palaeogeogr. Palaeoclimatol. Palaeoecol. 252, 617–625.

Zhou, B., Shen, C.D., Sun, W.D., Bird, M., Ma, W.T., Taylor, D., Liu, W.G., Peterse, F., Yi, W.X., Zheng, H.B., 2014. Late Pliocene–Pleistocene expansion of C4 vegetation in semiarid East Asia linked to increased burning. Geology 42 (12), 1067–1070.